

Electrochemical performance of Al-substituted $\text{Li}_3\text{V}_2(\text{PO}_4)_3$ cathode materials synthesized by sol-gel method

ZHANG Bao(张 宝)¹, LIU Jie-qun(刘洁群)^{1,2}, ZHANG Qian(张 倩)^{3,4}, LI Yan-hong(李艳红)⁵

1. School of Metallurgical Science and Engineering, Central South University, Changsha 410083, China;
2. Key Laboratory of New Processing Technology for Nonferrous Metals and Materials, Ministry of Education, Guilin University of Technology, Guilin 541004, China;
3. Guangxi Key Laboratory of Environmental Engineering, Protection and Assessment, Guilin University of Technology, Guilin 541004, China;
4. College of Environmental Science and Engineering, Guilin University of Technology, Guilin 541004, China;
5. Hunan Institute of Humanities, Science and Technology, Loudi 417000, China

Received 6 July 2009; accepted 29 January 2010

Abstract: The effect of Al-substitution on the electrochemical performances of $\text{Li}_3\text{V}_2(\text{PO}_4)_3$ cathode materials was studied. Samples with stoichiometric proportion of $\text{Li}_3\text{Al}_x\text{V}_{2-x}(\text{PO}_4)_3$ ($x=0, 0.05, 0.10$) were prepared by adding $\text{Al}(\text{NO}_3)_3$ in the raw materials of $\text{Li}_3\text{V}_2(\text{PO}_4)_3$. The XRD analysis shows that the Al-substituted $\text{Li}_3\text{V}_2(\text{PO}_4)_3$ has the same monoclinic structure as the un-substituted $\text{Li}_3\text{V}_2(\text{PO}_4)_3$. The SEM images show that Al-substituted $\text{Li}_3\text{V}_2(\text{PO}_4)_3$ has regular and uniform particles. The electrochemical measurements show that Al-substitution can improve the rate capability of cathode materials. The $\text{Li}_3\text{Al}_{0.05}\text{V}_{1.95}(\text{PO}_4)_3$ sample shows the best high-rate performance. The discharge capacity at 1C rate is 119 mA·h/g with 30th capacity retention rate about 92.97%. The electrode reaction reversibility and electronic conductivity are enhanced, and the charge transfer resistance decreases through Al-substitution. The improved electrochemical performances of Al-substituted $\text{Li}_3\text{V}_2(\text{PO}_4)_3$ cathode materials offer some favorable properties for their commercial application.

Key words: lithium ion batteries; cathode material; $\text{Li}_3\text{V}_2(\text{PO}_4)_3$; electrochemical performance; sol-gel method

1 Introduction

Since lithium iron phosphate was first reported as a cathode material for lithium-ion batteries, the framework materials based on the phosphate polyanion have recently been identified as potential electroactive materials for lithium and lithium ion batteries applications. Some other transition phosphate polyanion insertion hosts such as LiMnPO_4 [1], LiFePO_4 [2–5], LiVPO_4F [6–12], and $\text{Li}_3\text{V}_2(\text{PO}_4)_3$ [13–15] have received much attention because of their stable framework, relatively high voltage, good lithium ion transport and large theoretic capacity. With relatively high capacity and suitable operating voltage for the present commercial electrolyte system, $\text{Li}_3\text{V}_2(\text{PO}_4)_3$ is considered to be one of

the most promising cathode materials among the above-mentioned phosphate polyanion hosts. Monoclinic $\text{Li}_3\text{V}_2(\text{PO}_4)_3$ forms a three-dimensional (3D) framework that contains three independent lithium sites. However, a main drawback of pristine $\text{Li}_3\text{V}_2(\text{PO}_4)_3$ is its very low intrinsic electronic conductivity, which results in the poor rate performance. To solve this problem, various methods have been applied. The most successful approaches are cation substitution, particle size reduction and carbon coating on the surface of $\text{Li}_3\text{V}_2(\text{PO}_4)_3$ particles.

In the present work, a series of Al-substituted $\text{Li}_3\text{Al}_x\text{V}_{2-x}(\text{PO}_4)_3$ ($x=0, 0.05, 0.10$) cathode materials were synthesized to investigate the effects of Al substitution on the electrochemical properties of $\text{Li}_3\text{V}_2(\text{PO}_4)_3$.

Foundation item: Project(GuiJiaoRen[2007]71) supported by the Research Funds of the Guangxi Key Laboratory of Environmental Engineering, Protection and Assessment Program to Sponsor Teams for Innovation in the Construction of Talent Highlands in Guangxi Institutions of Higher Learning, China

Corresponding author: ZHANG Bao; Tel: +86-731-88836357; Fax: +86-731-88879469; E-mail: csuzb@vip.163.com
DOI: 10.1016/S1003-6326(09)60188-6

2 Experimental

$\text{Li}_3\text{Al}_x\text{V}_{2-x}(\text{PO}_4)_3$ ($x=0, 0.05, 0.10$) cathode materials were prepared by sol-gel route using $\text{LiOH}\cdot\text{H}_2\text{O}$, $\text{Al}(\text{NO}_3)_3$, NH_4VO_3 , H_3PO_4 and citric acid as raw materials in the molar ratio of $3:x:(2-x):3$ ($x=0, 0.05, 0.10$). The citric acid was dissolved in optimal distilled water, and then aqueous solution of $\text{Al}(\text{NO}_3)_3$, NH_4VO_3 and $\text{LiOH}\cdot\text{H}_2\text{O}$ were added respectively in sequence under continuous stirring. The obtained sol darkened after adding H_3PO_4 . In order to make metal ions chelated by citric acid thoroughly, the pH value of sol was adjusted to about 9.5 using $\text{NH}_3\cdot\text{H}_2\text{O}$ until the solution color gradually turned brown. After evaporating water at $80\text{ }^\circ\text{C}$, the as-prepared brown sol became gel. The gel was put into vacuum drying oven at $120\text{ }^\circ\text{C}$ for 6 h to expel H_2O and NH_3 as well as CO_2 due to part organic decomposing. The resulting product was then sintered at $650\text{ }^\circ\text{C}$ for 20 h under an inert atmosphere.

The X-ray diffractometer (XRD, XPert-Pro) measurement using Cu K_α radiation was employed and recorded at room temperature to identify the crystalline phase of the synthesized materials. The particle size and morphology of the $\text{Li}_3\text{V}_2(\text{PO}_4)_3$ powders were observed by scanning electron microscope (JEOL, GSM-6380 LV) with an accelerating voltage of 20 kV.

The electrochemical characterizations were performed using CR2025 coin-type cell. For positive electrode fabrication, the prepared powders were mixed with 10% of acetylene black and 10% of polyvinylidene fluoride in N-methyl pyrrolidinone until slurry was obtained. Then, the blended slurries were pasted onto an aluminum current collector. The electrode was dried at $120\text{ }^\circ\text{C}$ for 10 h in vacuum. The test cell consisted of the positive electrode and lithium foil negative electrode separated by a porous polypropylene film, and 1 mol/L LiPF_6 in EC:EMC:DMC (1:1:1 in volume) as the electrolyte. The assembly of the cells was carried out in a dry Ar-filled glove box. The cells were charged and discharged over a voltage range of 3.0–4.2 V versus Li/Li^+ electrode. The electrochemical impedance spectrum (EIS) measurements were performed in the frequency range of 10 kHz–10 mHz with an AC voltage of 5 mV.

3 Results and discussion

Fig.1 shows the XRD patterns for the prepared $\text{Li}_3\text{Al}_x\text{V}_{2-x}(\text{PO}_4)_3$ ($x=0, 0.05, 0.10$) cathode materials. It can be seen from Fig.1 that all samples are pure single phase with the monoclinic structure (space group $\text{P}2_1/\text{n}$). No other phases are detected in the XRD patterns, indicating that Al ions are completely substituted into the

crystal lattice of $\text{Li}_3\text{V}_2(\text{PO}_4)_3$. Al-substitution does not change the basic crystal structure of $\text{Li}_3\text{V}_2(\text{PO}_4)_3$.

The SEM images of $\text{Li}_3\text{Al}_x\text{V}_{2-x}(\text{PO}_4)_3$ ($x=0, 0.05, 0.10$) samples are shown in Fig.2. The Al-free $\text{Li}_3\text{V}_2(\text{PO}_4)_3$ has irregular particles. With increasing Al content, the primary particle size gradually increases and the shapes of the primary particles obviously are changed.

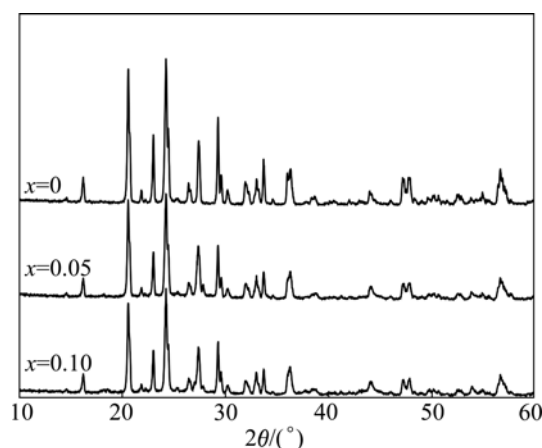


Fig.1 XRD patterns of $\text{Li}_3\text{Al}_x\text{V}_{2-x}(\text{PO}_4)_3$ ($x=0, 0.05, 0.10$)

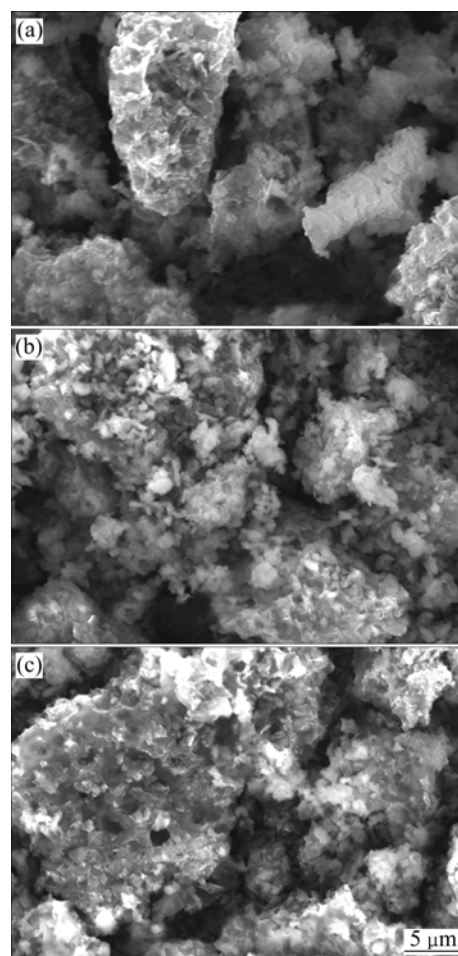


Fig.2 SEM images of $\text{Li}_3\text{Al}_x\text{V}_{2-x}(\text{PO}_4)_3$: (a) $x=0$; (b) $x=0.05$; (c) $x=0.10$

The electronic conductivities of the typical $\text{Li}_3\text{Al}_x\text{V}_{2-x}(\text{PO}_4)_3$ ($x=0, 0.05, 0.10$) powders were measured by a four-point conductivity test method, and the data are listed in Table 1. $\text{Li}_3\text{Al}_{0.05}\text{V}_{1.95}(\text{PO}_4)_3$ shows the highest electronic conductivity among all samples. The electronic conductivity of $\text{Li}_3\text{Al}_{0.05}\text{V}_{1.95}(\text{PO}_4)_3$ can reach 1.9×10^{-7} S/cm, about a factor of 10^2 higher than that of $\text{Li}_3\text{V}_2(\text{PO}_4)_3$. Lithium insertion and extraction in $\text{Li}_3\text{V}_2(\text{PO}_4)_3$ electrodes are accompanied by the electron transfer not only on the particle surface but also inside the crystals. Because the substitution effect induces the increase of semiconductivity of $\text{Li}_3\text{V}_2(\text{PO}_4)_3$, which enhances the electronic conductivity of the electrode materials on the crystal level, electron transfer in $\text{Li}_3\text{Al}_{0.05}\text{V}_{1.95}(\text{PO}_4)_3$ would be more facilitated than that in pure $\text{Li}_3\text{V}_2(\text{PO}_4)_3$.

Table 1 Electronic conductivity of $\text{Li}_3\text{Al}_x\text{V}_{2-x}(\text{PO}_4)_3$ ($x=0, 0.05, 0.10$) (S/cm)

$\text{Li}_3\text{V}_2(\text{PO}_4)_3$	$\text{Li}_3\text{Al}_{0.05}\text{V}_{1.95}(\text{PO}_4)_3$	$\text{Li}_3\text{Al}_{0.1}\text{V}_{1.9}(\text{PO}_4)_3$
2.1×10^{-8}	1.9×10^{-6}	1.2×10^{-6}

The electrochemical cycling performance of $\text{Li}_3\text{Al}_x\text{V}_{2-x}(\text{PO}_4)_3$ ($x=0, 0.05, 0.10$) samples are shown in Fig.3. The electrochemical cycling performances of $\text{Li}_3\text{Al}_x\text{V}_{2-x}(\text{PO}_4)_3$ ($x=0, 0.05, 0.10$) samples are evaluated in the $\text{Li}/\text{Li}_3\text{V}_2(\text{PO}_4)_3$ cell configuration at room temperature in the voltage range of 3.0–4.2 V at 0.5C charge rate and different discharge rates. From Fig.3, it can be seen that the specific capacities of the $\text{Li}_3\text{Al}_x\text{V}_{2-x}(\text{PO}_4)_3$ ($x=0.05, 0.10$) samples at 1C and 2C discharge rates are basically higher than that of un-substituted $\text{Li}_3\text{V}_2(\text{PO}_4)_3$. And the $\text{Li}_3\text{Al}_{0.05}\text{V}_{1.95}(\text{PO}_4)_3$ demonstrates remarkably improving specific capacity and cycling performance. For example, at 1C and 2C discharge rates, after 30 cycles the specific capacities of the un-substituted $\text{Li}_3\text{V}_2(\text{PO}_4)_3$ are smaller than 108 and 98 mA·h/g, with 30th capacity retention about 85.71% and 81.67%, respectively. Whereas the similar values of the $\text{Li}_3\text{Al}_{0.05}\text{V}_{1.95}(\text{PO}_4)_3$ are 119 and 110 mA·h/g, with 30th capacity retention about 92.97% and 88.0%, respectively. This result is expected because of the higher electronic conductivity of Al-substituted $\text{Li}_3\text{V}_2(\text{PO}_4)_3$ compared with the un-substituted $\text{Li}_3\text{V}_2(\text{PO}_4)_3$. This confirms that Al-substitution can affect the high-rate cycling performance of the $\text{Li}_3\text{Al}_x\text{V}_{2-x}(\text{PO}_4)_3$. Therefore, the substituted samples represent better electrochemical performance at high rate. When both high initial capacity and capacity retention rate are considered, $\text{Li}_3\text{Al}_{0.05}\text{V}_{1.95}(\text{PO}_4)_3$ shows the best electrochemical behavior than the other samples. This indicates that the diffusion of lithium ions is improved by

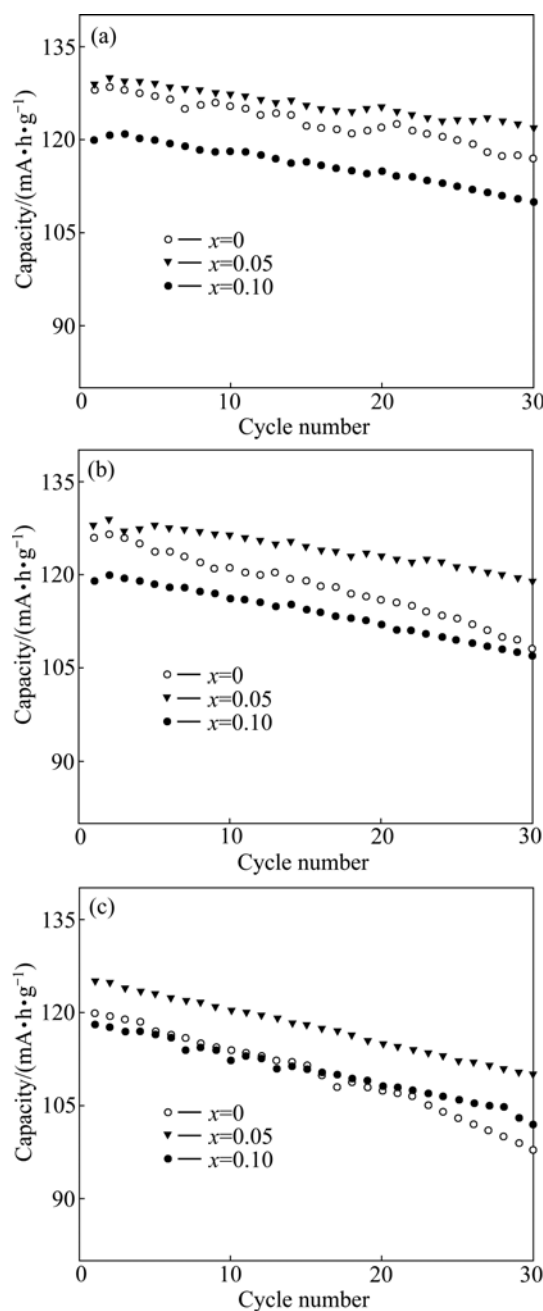


Fig.3 Cycling performance of $\text{Li}_3\text{Al}_x\text{V}_{2-x}(\text{PO}_4)_3$ at different discharge rates: (a) 0.5C; (b) 1C; (c) 2C

Al-substitution.

The effects of Al-substitution on the electrochemical performance of $\text{Li}_3\text{V}_2(\text{PO}_4)_3$ materials can be further understood by the first charge-discharge curves and electrochemical impedance spectra (EIS). Fig.4 shows the first charge-discharge curves of $\text{Li}_3\text{V}_2(\text{PO}_4)_3$, $\text{Li}_3\text{Al}_{0.05}\text{V}_{1.95}(\text{PO}_4)_3$, and $\text{Li}_3\text{Al}_{0.1}\text{V}_{1.9}(\text{PO}_4)_3$ at the rate of 0.5C in the voltage range of 3.0–4.2 V. As seen in Fig.5, it is clear that the initial charge capacities of $\text{Li}_3\text{V}_2(\text{PO}_4)_3$, $\text{Li}_3\text{Al}_{0.05}\text{V}_{1.95}(\text{PO}_4)_3$, and $\text{Li}_3\text{Al}_{0.1}\text{V}_{1.9}(\text{PO}_4)_3$ are about 136, 135 and 133 mA·h/g, respectively, and the

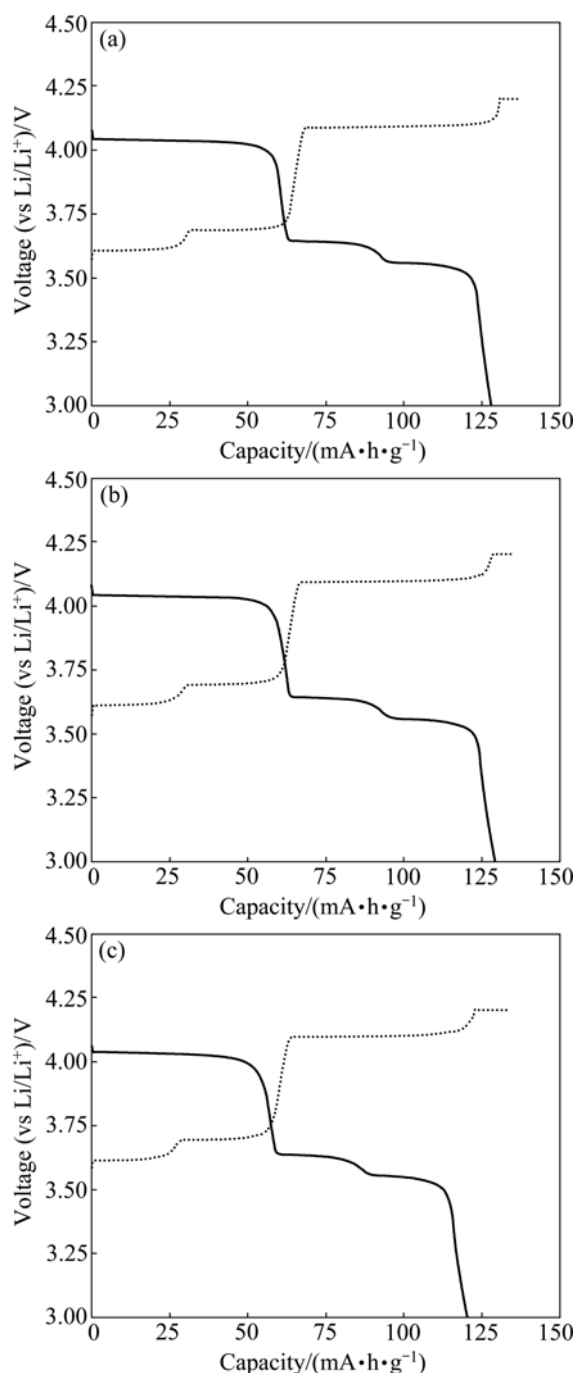


Fig.4 First charge-discharge curves of $\text{Li}_3\text{Al}_x\text{V}_{2-x}(\text{PO}_4)_3$: (a) $x=0$; (b) $x=0.05$; (c) $x=0.10$

discharge capacities are about 128, 129 and 120 $\text{mA}\cdot\text{h}/\text{g}$, respectively. The corresponding coulombic efficiency is 94.12%, 95.56% and 90.23%, respectively. It is clear that the electrode reaction reversibility is enhanced considerably when the mole fraction of Al (x) is 0.05.

The electrochemical impedance spectra (EIS) of $\text{Li}_3\text{V}_2(\text{PO}_4)_3$ and $\text{Li}_3\text{Al}_{0.05}\text{V}_{1.95}(\text{PO}_4)_3$ electrode materials were measured at different charging states. The typical Nyquist plots of EIS are presented in Fig.5 for both samples. Similar EIS patterns are observed for both samples. A semicircle is observed to center on the real

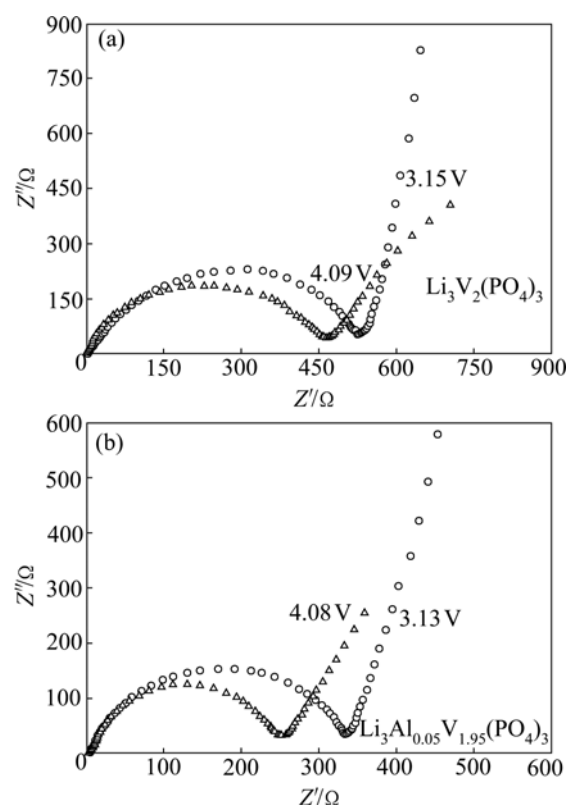


Fig.5 Nyquist plots for EIS of $\text{Li}_3\text{V}_2(\text{PO}_4)_3$ (a) and $\text{Li}_3\text{Al}_{0.05}\text{V}_{1.95}(\text{PO}_4)_3$ (b) at different charge states

axis at the high frequency range. In the low frequency range, a straight line with an angle of about 45° to the real axis corresponds to the Warburg impedance. The high frequency semicircle is related to the charge-transfer resistance (R_{ct}) and the double-layer capacitance. The low frequency tails result from the diffusion of lithium ions in the bulk active mass. In the case of $\text{Li}_3\text{Al}_{0.05}\text{V}_{1.95}(\text{PO}_4)_3$, the diameter of the semicircle significantly depends on the potential during charging, indicating that the film formation process is dependent on the lithium ion content. On the other hand, the charge-transfer resistance shows a greater dependence on the lithium insertion and extraction levels. In the highly charged states, the sample is found to deliver lower R_{ct} values. Comparing the diameter of the semicircle of the above two systems, it can be found that $\text{Li}_3\text{Al}_{0.05}\text{V}_{1.95}(\text{PO}_4)_3$ shows lower R_{ct} value than $\text{Li}_3\text{V}_2(\text{PO}_4)_3$, indicating that Al-substitution may cause some defects in the $\text{Li}_3\text{V}_2(\text{PO}_4)_3$ system, increase the electronic conductivity and improve the Li^+ kinetic behaviors.

4 Conclusions

1) Al-substituted $\text{Li}_3\text{Al}_x\text{V}_{2-x}(\text{PO}_4)_3$ ($x=0, 0.05, 0.10$) cathode materials are synthesized by sol-gel method.

2) The XRD analysis shows that Al-substituted $\text{Li}_3\text{V}_2(\text{PO}_4)_3$ has the same monoclinic structure as the un-substituted $\text{Li}_3\text{V}_2(\text{PO}_4)_3$. The SEM images of Al-substituted $\text{Li}_3\text{V}_2(\text{PO}_4)_3$ has regular and uniform particles.

3) The Al-substituted $\text{Li}_3\text{V}_2(\text{PO}_4)_3$ has higher discharge capacity and better charge/discharge cyclic stability. The $\text{Li}_3\text{Al}_{0.05}\text{V}_{1.95}(\text{PO}_4)_3$ sample shows the best high-rate performance. $\text{Li}_3\text{Al}_{0.05}\text{V}_{1.95}(\text{PO}_4)_3$ exhibits a discharge capacities about 119 mA·h/g and 110 mA·h/g at 1C and 2C discharge rates, with 30th capacity retention rate about 92.97% and 88.0%, respectively. In the Al-substituted $\text{Li}_3\text{V}_2(\text{PO}_4)_3$ system, the electrode reaction reversibility and electronic conductivity are enhanced, the charge-transfer resistance is decreased due to Al-substitution. In summary, the demonstrated performance of the prepared Al-substituted $\text{Li}_3\text{V}_2(\text{PO}_4)_3$ material offers some favorable properties for their commercial application.

References

- [1] CHEN Q Q, WANG J M, TANG Z, HE W C, SHAO H B, ZHANG J Q. Electrochemical performance of the carbon coated $\text{Li}_3\text{V}_2(\text{PO}_4)_3$ cathode material synthesized by a sol-gel method [J]. *Electrochim Acta*, 2007, 52(16): 5251–5257.
- [2] ZHONG S K, YIN Z L, WANG Z X, CHEN Q Y. Cathode material $\text{Li}_3\text{V}_2(\text{PO}_4)_3$: Low temperature solid-state reaction synthesis and performance [J]. *Inorg Chem*, 2006, 22(10): 1843–1846. (In Chinese)
- [3] LI Y Z, LIU X, YAN J. Study on synthesis routes and their influences on chemical and electrochemical performances of $\text{Li}_3\text{V}_2(\text{PO}_4)_3/\text{carbon}$ [J]. *Electrochim Acta*, 2007, 53(2): 473–479.
- [4] BARKER J, SAIDI M Y, SWOYER J L. Lithium metal fluorophosphates materials and preparation thereof [P]. US Patent, 2002–04–26.
- [5] ZHONG S K, YIN Z L, WANG Z X, CHEN Q Y. Synthesis and characterization of the triclinic structural LiVPO_4F as possible 4.2 V cathode materials for lithium batteries [J]. *Cent South Univ Techno*, 2007, 14(3): 340–343.
- [6] LI Y Z, ZHOU Z, GAO X P, YAN J. A novel sol–gel method to synthesize nanocrystalline LiVPO_4F and its electrochemical Li intercalation performances [J]. *J Power Sources*, 2006, 160(1): 633–637.
- [7] BARKER J, SAIDI M Y, SWOYER J L. Electrochemical insertion properties of the novel lithium vanadium fluorophosphates, LiVPO_4F [J]. *J Electrochem Soc*, 2003, 150(10): A1394–A1398.
- [8] BARKER J, SAIDI M Y, SWOYER J. A comparative investigate of the Li insertion properties of the novel fluorophosphates phases, NaVPO_4F and LiVPO_4F [J]. *Electrochem Soc*, 2004, 151(10): A1670–A1677.
- [9] BARKER J, SAIDI M Y, GOVER R K B, BURNS P, BRYAN A. The effect of Al substitution on the lithium insertion properties of lithium vanadium fluorophosphate, LiVPO_4F [J]. *J Power Sources*, 2007, 174(2): 927–931.
- [10] BARKER J, GOVER R K B, BURNS P, BRYAN A, SAIDI M Y, SWOYER J L. Structural and electrochemical properties of lithium vanadium fluorophosphates, LiVPO_4F [J]. *J Power Sources*, 2005, 146(1/2): 516–520.
- [11] CHEN J M, HSU C H, LI Y R, HSIAO M H. High-power LiFePO_4 cathode materials with a continuous nano carbon network for lithium-ion batteries [J]. *J Power Sources*, 2008, 184(2): 498–502.
- [12] JIN B, JIN E M, HEE K, GU H B. Electrochemical properties of LiFePO_4 -multiwalled carbon nanotubes composite cathode materials for lithium polymer battery [J]. *Electrochem Commun*, 2008, 10(10): 1537–1540.
- [13] HIROSE K, HONMA T, DOI Y, HINATSU Y, KOMATSU T. Mössbauer analysis of Fe ion state in lithium iron phosphate glasses and their glass-ceramics with olivine-type LiFePO_4 crystals [J]. *Solid State Commun*, 2008, 146(5/6): 273–277.
- [14] MI C H, ZHANG X G, ZHAO X B, LI H L. Effect of sintering time on the physical and electrochemical properties of LiFePO_4/C composite cathodes [J]. *J Alloys Compd*, 2006, 424(1/2): 327–333.
- [15] FANG H S, LI L P, LI G S. Hydrothermal synthesis of electrochemically active LiMnPO_4 [J]. *Chem Lett*, 2007, 36(3): 436–437.

(Edited by LI Xiang-qun)